Electronic Supplementary Material (ESI) for Journal of Materials Chemistry A.
This journal is © The Royal Society of Chemistry 2018

Supporting Information for

Activity Enhancement via Borate Incorporation in a NiFe (Oxy)hydroxide Catalysts for Electrocatalytic Oxygen Evolution

Experimental Section

Synthesis of the NiFe-borate catalyst

Chemicals

Iron-(III) chloride ($FeCl_3$), nickel-(II) chloride hexahygrate ($NiCl_6 \cdot 6H_2O$), sodium borate ($Na_2B_4O_7$), ethanol (≥99.5%), propylene oxide (≥99%) and Nafion solution (5wt%) were purchased from Sigma-Aldrich. All chemicals were used as received without further purification.

Synthesis of gelled NiFe-borate

The NiFe-borate catalysts was prepared by a room temperature sol-gel method. In a typical reaction, 2.1 mmol of $NiCl_6 \cdot 6H_2O$, 0.35 mmol of anhydrous $FeCl_3$, and 0.35 mmol of $Na_2B_4O_7$ were first dissolved in ethanol (2 mL) in a vial. Meanwhile, 1.8 ml of deionized water (DI) in 2 mL ethanol was prepared in a separate vial. The abovementioned solutions were cooled in an ice bath for 2 h to prevent uncontrolled hydrolysis. The Ni, Fe and B precursors were then mixed with the ethanol-water solution, and 1ml of propylene oxide was slowly added to the mixture to form a gel. The NiFe-borate wet-gel was aged for 24 h to facilitate network structure formation,

and then immersed in acetone for 5 days before the gel was cleaned and vacuum dried.

Characterization

An FEI SEM operated at 1.5 kV was used to characterize the surfaces of the samples. TEM and EELS elemental maps were taken on a Philips, FEI CM12 instrument. The samples were prepared by dropping catalyst powder dispersed in ethanol onto carbon-coated copper TEM grids using a micropipettes and drying under ambient conditions. XRD patterns were obtained with an instrument. Data were collected in Bragg Brentano mode using 0.02° divergence with a scan rate of 0.1 ° s^{-1}. Nitrogen BET surface area measurements were performed to determine the specific surface areas of the catalysts. N_2 adsorption-desorption isotherms of the catalysts were measured at -196 °C using a TriStar II Plus. The samples were outgassed under vacuum for 10 h at 100 °C prior to the measurements. The chemical state of the samples was investigated using XPS, (Thermo ESCALAB 250). The Ni K-edge EXAFS data were collected on the 1W1B beamline at the Beijing Synchrotron Radiation facility. Ni K-edge and Fe K-edge EXAFS spectra were recorded from 8.320 keV to 8.420 keV and 7.100 keV to 7.250 keV in fluorescence mode, respectively. All samples for measurements were prepared by depositing a thin film of the sample on carbon paper.

Electrochemical measurements

Electrochemical measurements were performed using a three-electrode system connected to an electrochemical workstation (Autolab PGSTAT302N) with a built-in EIS analyzer. The working electrode was a GCE (diameter: 3 mm, area: 0.072 cm^2)

from CH Instruments. Ag/AgCl (with saturated KCl as the filling solution) and platinum foil were used as the reference and counter electrodes, respectively.

Typically, 4 mg of catalyst powder was dispersed in a mixture of water (1 mL) and ethanol (0.25 mL), and then a Nafion solution (80 μL, 5 wt% in water) was added to the mixture. Then, a homogeneous ink was prepared by immersing the suspension in an ultrasonic bath for 30 min. The working electrode was prepared by dipping the GCE into the catalyst ink (catalyst loading 0.21 mg cm^{-2}).

To load the catalyst on Ni foam (thickness: 1.6 mm, Sigma), 20 mg of catalyst was dispersed in a mixture of water (2 ml) and ethanol (2 ml), and 100μL of Nafion solution was added. Then, the suspension was sonicated for 30 min to produce a homogeneous ink. Finally, 20 uL of the catalyst ink was drop-casted on a section of Ni foam with a fixed area of 0.5 × 0.5 cm^2 that was coated with water-resistant silicone glue.

Cyclic voltammetry (CV) measurements were performed for each sample at 50 mV s^{-1} for 10 cycles prior to performing LSV at 1 m V s^{-1}. EIS measurements were conducted in a static solution at 1.33 V (vs. RHE) on a GCE. The amplitude of the sinusoidal wave was 10 mV, and the frequency scan range was from 100 kHz to 1 Hz. Unless otherwise stated, all experiments were performed at ambient temperature (22±2 °C), and the electrode potential was converted to the RHE scale using the equation

$$E(RHE) = E(Ag/AgCl) + 0.197\,V + 0.059 * pH \quad (1)$$

Density Functional Theory (DFT) Calculation Setup

The Ni (Oxy)hydroxide model was constructed based on the β-NiOOH structure. Following the previous studies,[1-3] we have the (0001) facet of the NiOOH exposed to

the vacuum. The calculations were performed using the DFT+U scheme, where the U = 6.2 eV for Ni and 5.3 eV for Fe, following the setup on the Material Project website. The system contains three layers of the NiOOH along the z-axis, and it has 4×3 unit cells within the x-y plane. The electron was described using the Perdew-Burke-Ernzerhof (PBE) level[4] of the DFT theory using the projector augmented-wave method,[5] with a 520 eV cutoff. The vdW interactions were described using the Grimme's dispersion correction with the Becke-Jonson damping.[6] All the calculations were performed using the VASP package.[7]

As it is demonstrated in the previous reports, the protonation state of the Ni (Oxy)hydroxide systems can be extremely complicated.[8,9] However, this is not the main focus of the current study, and we have the system spontaneously relaxed to the current structure. Hence, the calculation is mainly to demonstrate a trend supported by the experimental characterizations. We did compare the relative binding energy (**Fig. S7**). The configuration with a lower energy was chosen in the main text.

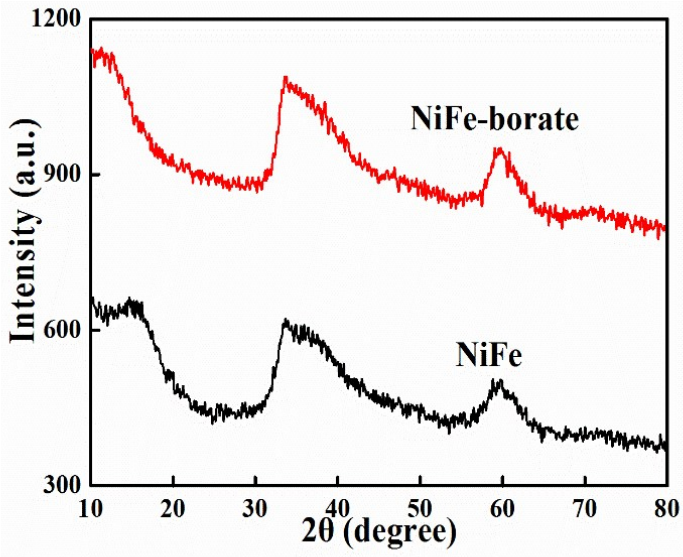

Figure S1. XRD patterns of NiFe-borate and the control, which illustrate the weakly crystalline character.

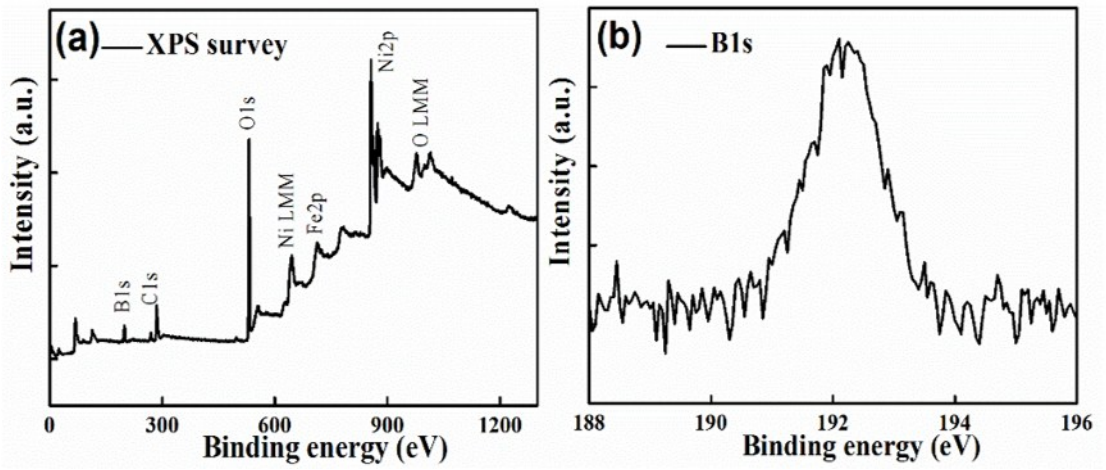

Figure S2. XPS analysis. (a) Survey XPS spectrum and (b) high-resolution B1s XPS spectrum of NiFe-borate.

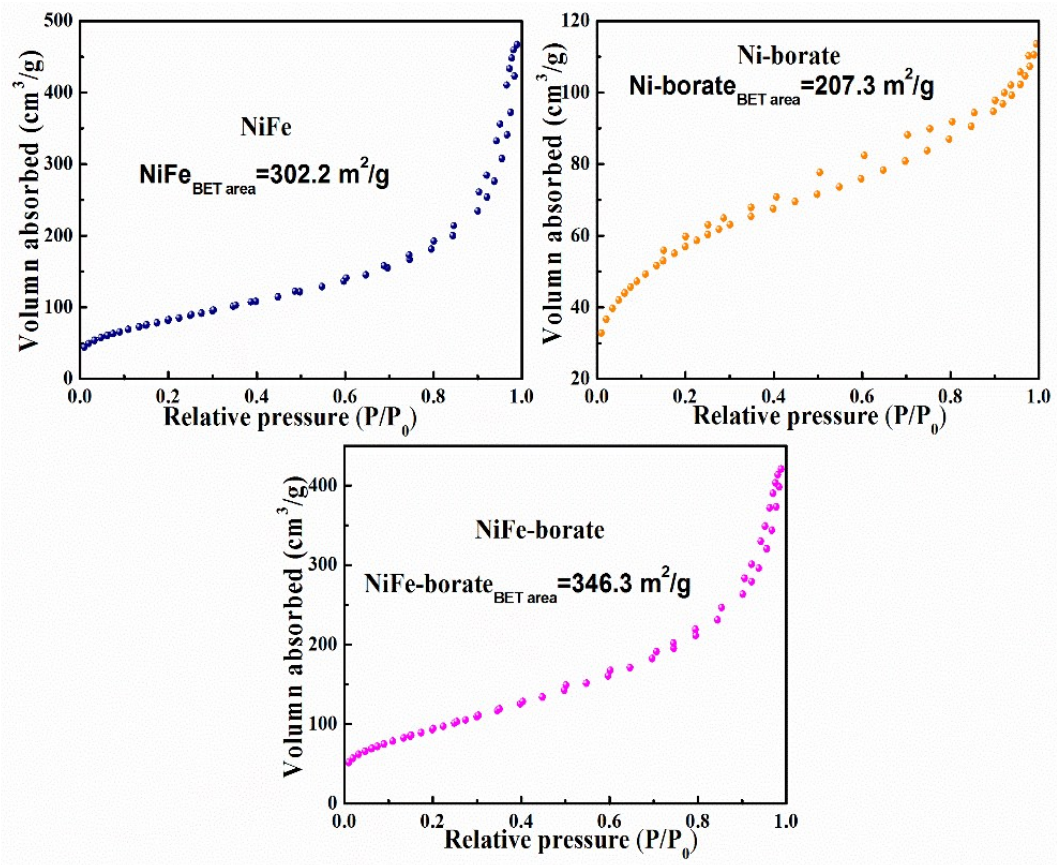

Figure S3. BET surface area analysis. N_2 sorption isotherms of NiFe-borate, Ni-borate and NiFe.

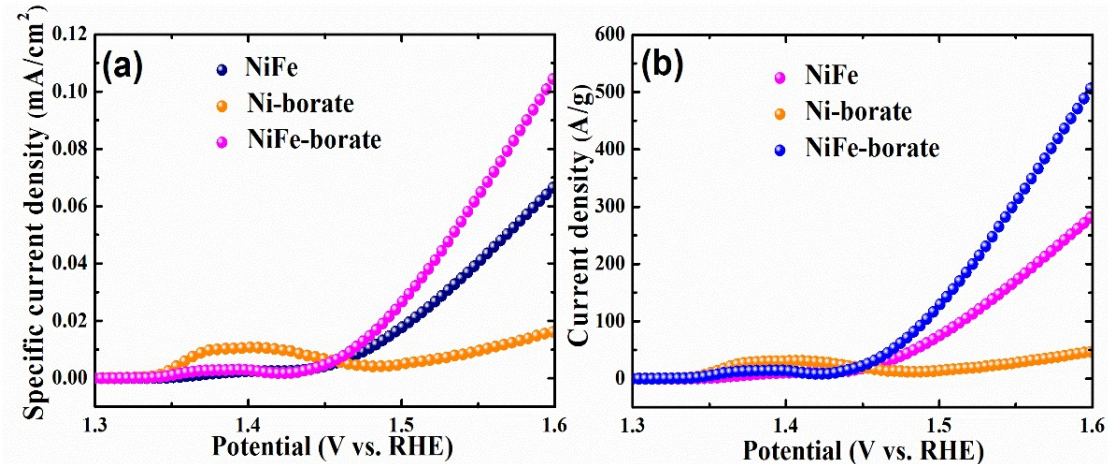

Figure S4. Characterization of the intrinsic activity of the catalysts on a GCE in 1 M KOH electrolyte. OER polarization curves normalized to (a) the BET surface area and (b) the catalyst mass of NiFe-borate and the controls.

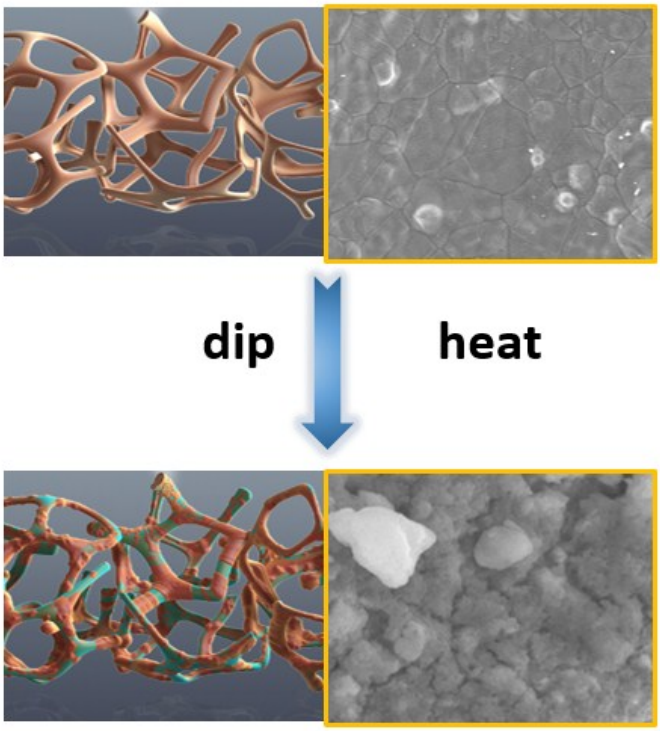

Figure S5. Schematic illustration of the preparation process and the SEM morphology on Ni foam.

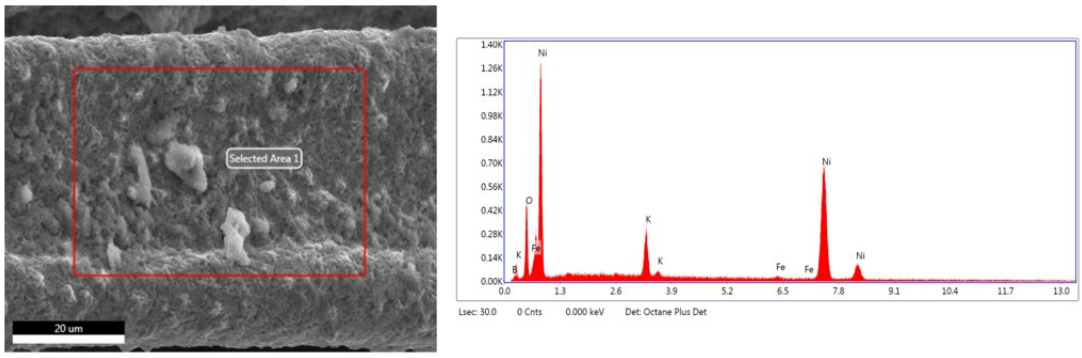

Figure S6. The SEM and EDS analyses of NiFe-borate show that a similar porous nanostructured morphology and the elements Ni, Fe and B are maintained in the catalyst after the 110-hours stability test.

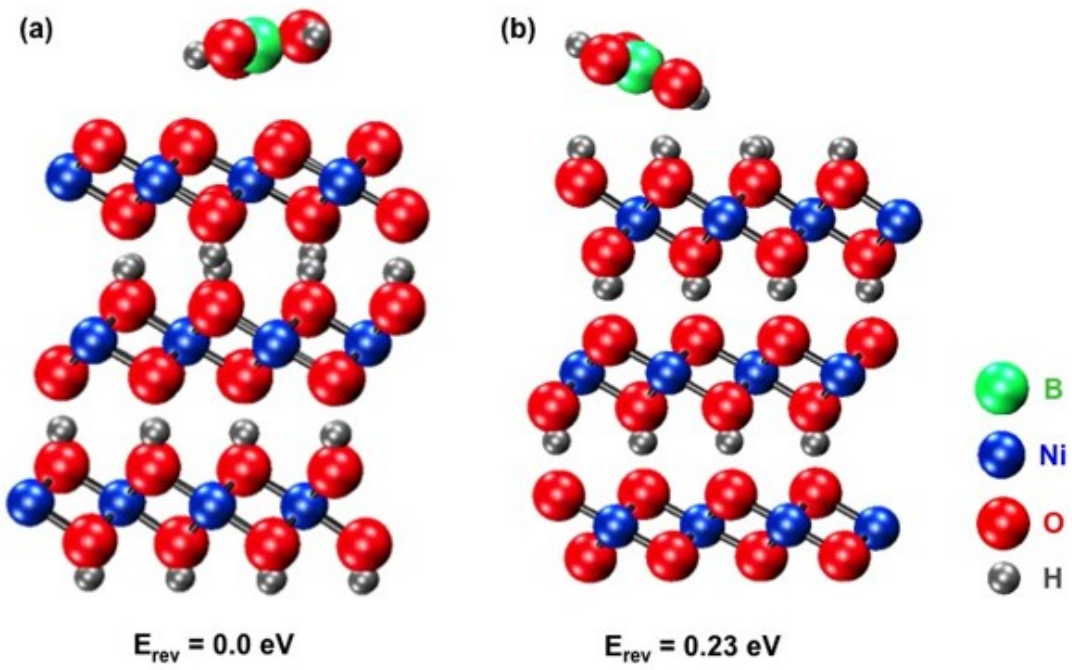

Figure S7. DFT optimized borate-mediated Ni (oxyhydroxide) catalyst. We choose the configuration with a lower energy in the main context.

Table S1 Comparison of the catalytic parameters for the NiFe-borate catalyst and the controls.

Sample	Electrolyte	On GCE (mV) (10 mA/cm^2)	On Ni Foam(mV) (10 mA/cm^2)	Reference
		Overpotential(mV)	Overpotential (mV)	
NiFe-borate	**1 M KOH**	**230**	**200**	**This work**
NiFe hydroxide	1 M KOH	240	-	*Adv. Energy Mater.* **2017**[10]
$Na_{1-x}Ni_yFe_{1-y}O_2$	1 M KOH	-	260	*Energy Environ. Sci.* **2017**[11]
NiFe hydroxide	1 M KOH	210	-	*Adv. Mater.* ***2017***[12]
NiFe/NC	1 M KOH	330	-	*ACS Catal.* **2016**[13]
NiFeO	0.1 M KOH	320	-	*J. Am. Chem. Soc.* **2016**[14]
Ni_3FeN-NP	1 M KOH	280	-	*Adv. Energy Mater.* **2016**[15]
NiFeCo	0.1 M KOH	340	-	*Adv. Energy Mater.* **2016**[16]
NiCoFe	1 M KOH	-	230[a]	*ACS Energy Lett.* **2016**[17]
$LiCo_{0.33}Ni_{0.33}Fe_{0.33}O_2$	0.1 M KOH	240[a]	-	*Nat. Commun.* **2014**[18]
NiFeMn	1 M KOH		200[b]	*Energy Environ. Sci.* **2016**[19]
NiFe	1 M KOH	-	240	*Nat. Commun.* **2015**[20]
NiFeO	0.1 M KOH	250[a]	-	*Nat. Commun.* **2015**[21]

a. on carbon fiber cloth

b. free-standing

References

1. A. J. Tkalych, K. Yu and E. A. Carter, *J. Phys. Chem. C*, 2015, **119**, 24315.

2. D. K. Bediako, Y. Surendranath and D. G. Nocera, *J. Am. Chem. Soc.*, 2013, **135**, 3662.

3. A. Tkalych , J. M. P. Martirez and E. A. Carter, *Phys. Chem. Chem. Phys.,* 2018. (new accept)

4. J.P. Perdew, K. Burke and M. Ernzerhof, *Phys. Rev. B*, 1996, **77**, 3865.

5. P.E. Blöchl, *Phys. Rev. B*, 1994, **50**, 17953.

6. S. Grimme, J. Antony, S. Ehrlich and H. Krieg, *J. Chem. Phys.*, 2010, **132**, 154104.

7. G. Kresse, G. Kresse and D. Joubert, *Phys. Rev. B*, 1999, **59**, 1758.

8. Y. Elbaz and M. C. Toroker, *J. Phys. Chem. C*, 2017, **121**, 16819.

9. J. C. Conesa, *J. Phys. Chem. C*, 2016, **120**, 18999.

10. W. Zhang, Y. Wu, J. Qi, M. Chen and R. Cao, *Adv. Energy Mater.*, 2017, **7**, 1602547.

11. B. Weng, F. Xu, C. Wang, W. Meng, C. R. Grice and Y. Yan, *Energy Environ. Sci.*, 2017, **10**, 121.

12. Y. Jia, L. Zhang, G. Gao, H. Chen, B. Wang, J. Zhou, M. T. Soo, M. Hong, X. Yan, G. Qian, J. Zou, A. Du and X. Yao, *Adv. Mater.,* 2017, **29**, 1700017.

13. X. Zhang, H. Xu, X. Li, Y. Li, T. Yang, and Y. Liang, *ACS Catal.*, 2016, **6**, 580.

14. M. Görlin, P. Chernev, J. Ferreira de Araújo, T. Reier, S. Dresp, B. Paul, R. Krähnert, H. Dau and P. Strasser, *J. Am. Chem. Soc.*, 2016, **138**, 5603.

15. X. D. Jia, Y. F. Zhao, G. B. Chen, L. Shang, R. Shi, X. F. Kang, G. I. N. Waterhouse,

L. -Z. Wu, C.-H. Tung and T. R. Zhang, *Adv. Energy, Mater.*, 2016, **6**, 1502585.

16. L. Han, S. J. Dong and E. K. Wang, *Adv. Mater.*, 2016, **28**, 9266.

17. A. -L. Wang, H. Xu and G. R. Li, *ACS Energy Lett.*, 2016, **1**, 445.

18. Z. Y. Lu, H. T. Wang, D. Kong, K. Yan, P. -C. Hsu, G. Y. Zheng, H. B. Yao, Z. Liang, X. M. Sun and Y. Cui, *Nat. Commun.*, 2014, **5**, 4345.

19. E. Detsi, J. B. Cook, B. K. Lesel, C. L. Turner, Y.-L. Liang, S. Robbennolt and S. H. Tolbert, *Energy Environ. Sci.*, 2016, **9**, 540.

20. X. Lu and C. Zhao, *Nat. Commun.*, 2015, **6**, 6616.

21. H. T. Wang, H. -W. Lee, Y. Deng, Z. Y. Lu, P. -C. Hsu, Y. Y. Liu, D. C. Lin and Y. Cui, *Nat. Commun.*, 2015, **6**, 7261.